Variational boundary element acoustic modelling over mixed quadrilateral–triangular element meshes

Ahlem Alia[1,*,†], Mhamed Souli[1] and Fouad Erchiqui[2]

[1]*LML, Boulevard Paul Langevin, Cité Scientifique, 59655 Villeneuve d'Ascq Cedex, France*
[2]*Université du Québec en Abitibi-Témiscamingue, 445 boul. de l'Université,*
Rouyn-Noranda QC, Que., Canada J9X 5E4

SUMMARY

The variational indirect boundary element method is widely used in many acoustical problems such as simulation of scattering and radiation phenomena. Although it has many advantageous features in dealing with those problems, it suffers from the singularity problem when the double surface integral is done over the same element. In this paper, a straightforward technique for computing the singularity $1/R$ over triangular element is presented. It is based on a generalized polar co-ordinates transformation to transform the triangular master element into a square one. The singularity factor is taken as weight function. Consequently, a single straightforward implementation without any special treatment of singularity is possible for meshes involving both quadrilateral and triangular elements of higher order. The efficiency of the proposed method is demonstrated for some numerical examples. Copyright © 2006 John Wiley & Sons, Ltd.

KEY WORDS: variational indirect boundary element method; singularity; triangles; polar co-ordinate transformation

1. INTRODUCTION

The variational indirect boundary element method (VIBEM) [1–3] is extensively used in numerical acoustics especially for solving radiation and scattering problems in infinite domains. In fact, it can handle automatically and exactly the Sommerfield radiation condition via fundamental solution of the Helmholtz equation. In addition, it leads to symmetric matrices due to the double surface integration. However, it suffers from the singularity problem which occurs when the double integral surface involves the same element. In the last years, many

efforts have been devoted to calculate efficiently the singular integrals without sacrificing any accuracy. In fact, special numerical treatment or analytical rearrangement of the resulting singular integrals is always needed in order to eliminate difficulties related to their integrability. On the other hand, various approaches, mixing numerical and analytical quadrature methods have been successfully developed; useful references are cited in Reference [4].

Hamdi [1], Erchiqui [2] and Tournour [3] computed the singular integrals semi-analytically over triangular elements. This approach is still limited for only elements with linear shape functions. Jeans and Mathews [5] divided quadratic element into four triangular subelements for each integration Gauss point. The singularity occurs at the corner of the subelements. In this case, the corresponding Jacobian relating the element to the subelement removes the singularity of the Green function. In the same manner, Chen *et al.* [6] subdivided the boundary element (triangles and quadrangles) into triangles such that the singular point becomes a corner of these subelements. Using triangular polar co-ordinates, the corresponding master element of these subelements can be transformed into a square of unit side length. Hence, the singular corner point of the triangular subelement becomes an edge of the unit square, on which non-singular integration can be performed. For singular integral, Bajaj *et al.* [7] adopted an integration technique based on a fine mesh around the singular point which is created by repeated subdivisions. The density of the mesh increases towards the singular points, and the method gives accurate results. However, these multiple subdivisions need more computational time. Wang and Atalla [8] proposed an algorithm for double surface integrals with a singularity of $1/R$ over quadrilateral elements. This technique involves a weighted type of integration where the singularity is taken into account in the weights. In contrast with classical methods [1–3, 5–7] which require special treatment for singularities, Wang and Atalla [8] describe a straightforward method for the implementation of the VIBEM for quadrilateral elements.

In this paper, Wang's method [8] is extended to triangular elements using a generalized polar co-ordinates transformation proposed by Wu [9]. Hence, meshes involving both triangular and quadrilateral elements with higher order can be handled by a single straightforward implementation without any special treatment of singularities.

2. GOVERNING EQUATIONS

Let us consider a boundary surface 'S' enclosing a volume 'Ω' filled and surrounded by an ideal and homogeneous fluid medium (Figure 1).

For a harmonic disturbance of frequency 'f' without any source or loss mechanisms, the pressure 'p' satisfies the Helmholtz equation:

$$\Delta p(x) + k^2 p(x) = 0 \tag{1}$$

where $k = \omega/c$ denotes the wave number, c is the sound velocity, $\omega = 2\pi f$ is the pulsation and x is the field point position. For Neumann boundary condition which implies that the velocity is continuous across the surface S:

$$\frac{\partial p}{\partial n} = -\mathrm{j}\rho\omega V_n \tag{2}$$
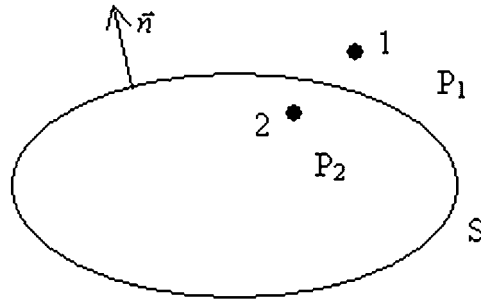
Figure 1. Acoustic domain and its boundary.

the pressure at any point within either one of the two acoustic domains can be expressed as follows:

$$p(x) = \int_{S_y} \mu(y) \frac{\partial G(x, y)}{\partial n_y} \, dS_y \tag{3}$$

where ρ is the fluid density, V_n is the normal velocity, $\mu = p_1 - p_2$ is the double potential layer, n_y is the unit normal at the location of the source point, $G = e^{-jkR}/4\pi R$ is the Green's function with $j = \sqrt{-1}$ and $R = \|x - y\|$ is the distance between the field point x and the source point y.

Equation (3) states that the sound pressure at any point inside the acoustic domain can be obtained by integrating the equation on the boundary. This is the main idea of the BEM in which only the boundary information is needed to obtain the solution. However, Equation (3) is not ready to be used because the double potential layer μ on the boundary is unknown. In order to find it, we applied in what follows the boundary condition on the surface of the acoustic domain.

By taking into account Neumann boundary condition given by Equation (2), an integral equation can be derived for the velocity from Equation (3).

$$-j\rho\omega V_n = HFP \int_{S_y} \mu(y) \frac{\partial^2 G(x, y)}{\partial n_x \partial n_y} \, dS_y \tag{4}$$

This integral over the single surface S_y, which is associated with the second derivative of the Green function, should be defined in the sense of Hadamard finite part (HFP) [4]. An increasing number of researchers have focused on hypersingularity and proposed both analytical and numerical techniques to handle it. A summary on regularization methods for hypersingularity can be found in Reference [10].

In order to solve simultaneously interior and exterior problems, we will associate to Equation (4) a variational formulation that presents a double advantage. First, it allows avoiding evaluation of HFP. On the other hand, it leads to a symmetric algebraic system.

The variational formulation can be derived by multiplying the integral equation (Equation (4)) by $\mu(x)$ and integrating it over the BE model with velocity boundary condition on S. This formulation is based on the principle that the solution of the obtained equation will

also minimize the following functional:

$$F(\mu) = 2 \int_{S_x} j\rho\omega\mu(x)V_n(x)\,dS_x + \int_{S_x}\left(\mu(x)\int_{S_y}\left(\frac{\partial^2 G(x,y)}{\partial n_x \partial n_y}\mu(y)\right)dS_y\right)dS_x \tag{5}$$

The singularity which appears in the functional F can be reduced to a less singular form that is better suited to numerical calculations [1–3]:

$$F(\mu) = 2\int_{S_x} j\rho\omega V_n(x)\mu(x)\,dS_x + \int_{S_x}\int_{S_y}(k^2(n_x.n_y)\mu_x\mu_y$$

$$- (\nabla_x\mu(x)\times n_x)(\nabla_y\mu(y)\times n_y))G(x,y)\,dS_y\,dS_x \tag{6}$$

By discretizing Equation (6) using BEM, the final numerical system is derived by imposing a stationary condition on F with respect to unknown primary variable μ. Solving the obtained system allows to get the double layer potential at the boundary. Consequently, Equation (3) can be used to compute the pressure at any point in the acoustic domain.

3. DISCRETIZATION

In order to achieve a numerical solution of Equation (6), the surface is divided into boundary elements such as

$$S \approx S^h = \bigcup_{i=1}^{\text{Elements}} S_i$$

$$\int_{S_x}(\ )\,dS_x = \sum_{i=1}^{\text{Elements}}\int_{S_x^i}(\ )\,dS_x^i \tag{7}$$

$$\int_{S_x}\int_{S_y}(\ )\,dS_y\,dS_x = \sum_{i=1}^{\text{Elements}}\sum_{j=1}^{\text{Elements}}\int_{S_x^i}\int_{S_y^j}(\ )\,dS_y^i\,dS_x^j$$

The double potential layers $\mu(x)$ and $\mu(y)$ on the surface of the boundary element model are expressed as a product between their unknown nodal values and the element shape functions as

$$\mu(y) = N_j(\xi_1,\eta_1)\mu_j$$
$$\mu(x) = N_i(\xi_2,\eta_2)\mu_i \tag{8}$$

with (ξ_1,η_1) and (ξ_2,η_2) represent, respectively, the local co-ordinates on the elements 'i' and 'j', $N_i(\xi_1,\eta_1)$ and $N_j(\xi_2,\eta_2)$ are the shape functions, x and y are position vectors on the elements 'i' and 'j'. For clarity, we drop the superscript 'h' in S^h.

In order to discretize the second term of Equation (6), we use Equation (9) that is proved in Reference [3]:

$$[n_x\times\nabla_x\mu][n_y\times\nabla_y\mu] = \mu_i\frac{1}{J_x}\{(x_{,\eta_1}.y_{,\eta_2})N_{i,\xi_1}N_{j,\xi_2} - (x_{,\eta_1}.y_{,\xi_2})N_{i,\xi_1}N_{j,\eta_2}$$

$$- (x_{,\xi_1}.y_{,\eta_2})N_{i,\eta_1}N_{j,\xi_2} + (x_{,\xi_1}.y_{,\xi_2})N_{i,\eta_1}N_{j,\eta_2}\}\frac{1}{J_y}\mu_j \tag{9}$$

where $x_{,\varsigma_1} = x_{,\xi_1} \times x_{,\eta_1}, y_{,\varsigma_2} = y_{,\xi_2} \times y_{,\eta_2}, J_x = \|x_{,\varsigma_1}\|$ and $J_y = \|y_{,\varsigma_2}\|$. The subscripts $,\xi_1$ $,\eta_1$ $,\varsigma_1$, ξ_2 $,\eta_2$ $,\varsigma_2$ are, respectively, the partial derivatives with respect to $\xi_1, \eta_1, \varsigma_1, \xi_2, \eta_2$ and ς_2. By replacing Equation (9) in the discretized form of Equation (6), and by using the fact that the area of infinitesimal surfaces are given by $dS_y^j = J_y \, d\xi_1 \, d\eta_1$ and $dS_x^i = J_x \, d\xi_2 \, d\eta_2$, the two terms of the discretized functional can be written as

$$\int_{S_x^j} \int_{S_y^i} (k^2(n_x.n_y)\mu_x\mu_y - (\nabla_y\mu(x) \times n_x)(\nabla_y\mu(y) \times n_y))G(x,y)\,dS_y^i\,dS_x^j = \mu_i a_{ij}\mu_j$$

$$- \int_{S_x^i} j\rho\omega\mu(x)V_n(x)\,dS_x^i = \mu_i b_i \qquad (10)$$

where

$$a_{ij} = \int_{\xi_2}\int_{\eta_2}\int_{\xi_1}\int_{\eta_1} G(x,y)\{k^2(x_{,\varsigma_1}.y_{,\varsigma_2})N_i(\xi_1,\eta_1)N_j(\xi_2,\eta_2) - (x_{,\eta_1}.y_{,\eta_2})N_{i,\xi_1}(\xi_1,\eta_1)N_{j,\xi_2}(\xi_2,\eta_2)$$

$$+ (x_{,\eta_1}.y_{,\xi_2})N_{i,\xi_1}(\xi_1,\eta_1)N_{j,\eta_2}(\xi_2,\eta_2) + (x_{,\xi_1}.y_{,\eta_2})N_{i,\eta_1}(\xi_1,\eta_1)N_{j,\xi_2}(\xi_2,\eta_2)$$

$$- (x_{,\xi_1}.y_{,\xi_2})N_{i,\eta_1}(\xi_1,\eta_1)N_{j,\eta_2}(\xi_2,\eta_2)\} \, d\xi_1 \, d\eta_1 \, d\xi_2 \, d\eta_2$$

$$= \int_{\xi_2}\int_{\eta_2}\int_{\xi_1}\int_{\eta_1} \frac{g(\xi_1,\eta_1,\xi_2,\eta_2)}{R} \, d\xi_1 \, d\eta_1 \, d\xi_2 \, d\eta_2 \qquad (11a)$$

$$b_i = -j\rho\omega \int_{\xi_2}\int_{\eta_2} N_i(\xi_2,\eta_2)V_n J_x \, d\xi_2 \, d\eta_2 = \int_{\xi_2}\int_{\eta_2} \vartheta(\xi_2,\eta_2) \, d\xi_2 \, d\eta_2 \qquad (11b)$$

Finally, the discretized form of the functional F (Equation (6)) noted F^h may then be written as

$$F^h = \sum_i \sum_j \mu_i a_{ij}\mu_j - 2\sum_i \mu_i b_i \qquad (12)$$

or in a matrix form:

$$F^h = \mu^T A\mu - 2\mu^T B \qquad (13)$$

F^h is a bilinear function of the unknown nodal potentials. Imposing stationary condition on F^h with respect to unknown primary variables μ

$$\frac{\partial F^h}{\partial \mu} = 0 \Rightarrow A\mu = B \qquad (14)$$

leads to the following system of equations:

$$A\mu = B \qquad (15)$$

where the global matrix A is resulting from assembling the elementary matrices a_{ij} and the right-hand side B results from assembling the elementary vectors b_i. The system matrix A is square and symmetric since it is derived using a variational formulation. Once the double potential layer is calculated by solving the linear system given by Equation (15), the acoustic pressure at any field point in the domain can be computed via integral equation (3). It is to be emphasized that the numerical integration over two different elements can be calculated

without any difficulty. However, when it involves only one element, a singularity appears. In this case, the singularity may be correctly evaluated in order to obtain good pressure.

4. NUMERICAL INTEGRATION

The purpose of this section is to process numerically triangular and quadrilateral elements into the same algorithm. To do so, master element of triangles is transformed into square element. Consequently, this transformation allows us to extend any quadrilateral element algorithm to a triangular one with only few modifications.

For triangular element, we first use the following generalized polar transformation in Reference [9] to transform the triangular master element into a unit side-length square:

$$\xi = \rho(1 - \theta)$$
$$\eta = \rho\theta \tag{16}$$

where $0 \leqslant \rho \leqslant 1, 0 \leqslant \theta \leqslant 1$ (Figure 2). The radial co-ordinate ρ is equal to zero at the origin of the generalized polar co-ordinate system (node 3 in Figure 2), and is equal to one
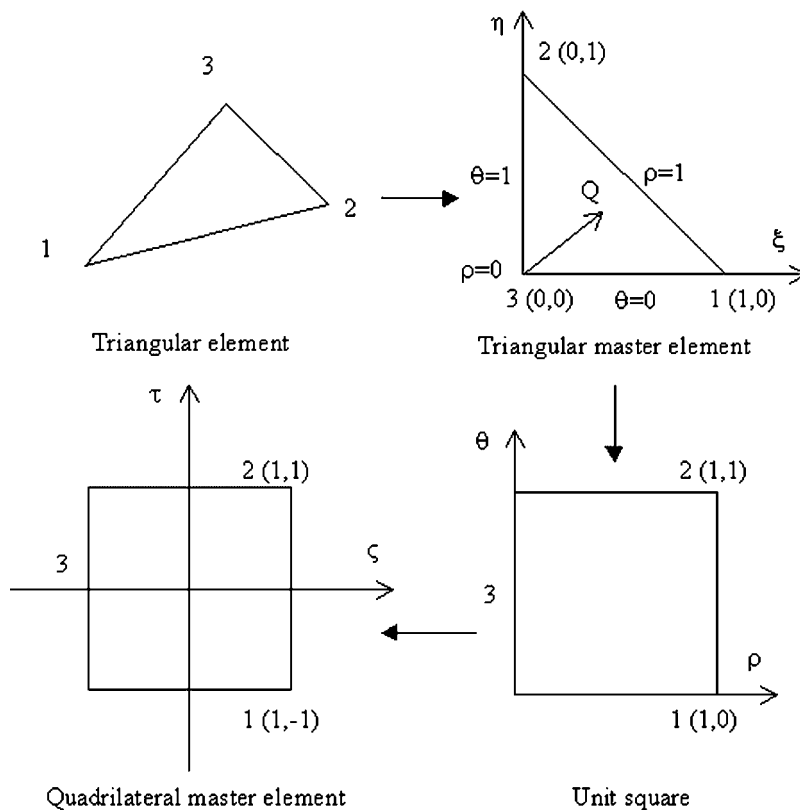

Figure 2. Generalized polar co-ordinate transformation.

at any point on the hypotenuse. The angle θ is equal to zero on the ξ-axis and is equal to one on the η-axis. This transformation, obtained from vectors addition, allows to get any point Q inside the parent element. We can show that the Jacobian of this transformation is equal to ρ. To transform the (1×1) square to (2×2) square, let us consider the following simple transformation:

$$\rho = \tfrac{1}{2}(1 + \tau)$$
$$\theta = \tfrac{1}{2}(1 + \zeta) \tag{17}$$

for which the Jacobian is equal to $\frac{1}{4}$. The global Jacobian of the two is given by $J = \rho/4$. Hence, the discretized form associated to a triangular master element could be rewritten over the corresponding square master element. Consequently, for meshes containing both triangular and quadrilateral elements, the corresponding integral can be rewritten as

$$a_{ij} = \int_{\xi_2} \int_{\eta_2} \int_{\xi_1} \int_{\eta_1} \frac{g(\xi_1, \eta_1, \xi_2, \eta_2)}{R} \, d\xi_1 \, d\eta_1 \, d\xi_2 \, d\eta_2$$

$$= \iiiint_{-1}^{1} \frac{g(\underline{\xi}_1, \underline{\eta}_1, \underline{\xi}_2, \underline{\eta}_2)}{R} J_1 J_2 \, d\underline{S}_1 \, d\underline{S}_2 \tag{18a}$$

$$b_i = \int_{\xi_2} \int_{\eta_2} \vartheta(\xi_2, \eta_2) \, d\xi_2 \, d\eta_2 = \iint_{-1}^{1} \vartheta(\underline{\xi}_2, \underline{\eta}_2) J_2 \, d\underline{S}_2 \tag{18b}$$

where

$$d\underline{S}_i = \begin{cases} d\xi_i \, d\eta_i & \text{if } (i) \text{ is quadrangle} \\ d\tau_i \, d\zeta_i & \text{if } (i) \text{ is triangle} \end{cases} \quad \text{with } i = 1, 2$$

$$\underline{\xi}_i = \begin{cases} \xi_i & \text{if } (i) \text{ is quadrangle} \\ \xi_i(\tau_i, \zeta_i) & \text{if } (i) \text{ is triangle} \end{cases}$$

and

$$J_i = \begin{cases} 1 & \text{if } (i) \text{ is quadrilateral element} \\ \dfrac{\rho_i}{4} & \text{if } (i) \text{ is triangular element} \end{cases}$$

When the double surface integral is done over different elements $(i \neq j)$, Gauss quadrature rule can be directly applied. However, when the integral involves the same element, it becomes singular. In this case, the Wang and Atalla [8] integration technique, proposed first for quadratic elements, can be easily extended to triangles since these ones are transformed above into square master elements. A simple way to distinguish a triangular element from a quadrilateral one is to define the triangle by a degenerated quadrangle where the last two nodes are identical. To extend a previous variational boundary quadrilateral element implementation to a mixed quadrilateral–triangular element meshes, Equations (16) and (17) can be easily developed and included in existing acoustic codes.

By denoting $r = \sqrt{(\underline{\xi}_1 - \underline{\xi}_2)^2 + (\underline{\eta}_1 - \underline{\eta}_2)^2}$ the distance over the master element and since r/R is bounded over the element [8], integral (18a) is equivalent to the following one:

$$a_{ij} = \iiiint_{-1}^{1} \frac{f(\underline{\xi}_1, \underline{\eta}_1, \underline{\xi}_2, \underline{\eta}_2)}{r} \, d\underline{S}_1 \, d\underline{S}_2 \qquad (19)$$

where $f(\underline{\xi}_1, \underline{\eta}_1, \underline{\xi}_2, \underline{\eta}_2) = (r/R)g(\underline{\xi}_1, \underline{\eta}_1, \underline{\xi}_2, \underline{\eta}_2)J_1 J_2$. By using the weighted integration [8] in which the factor of singularity in the integrand is taken as weight function W_{mnkl}, the last integral becomes

$$a_{ij} = \sum_{m=1}^{M_{\xi_1}} \sum_{n=1}^{M_{\eta_1}} \sum_{r=1}^{M_{\xi_2}} \sum_{l=1}^{M_{\eta_2}} f(\underline{\xi}_1^m, \underline{\eta}_1^n, \underline{\xi}_2^r, \underline{\eta}_2^l) W_{mnrl} \qquad (20)$$

where $M_{\xi_1}, M_{\eta_1}, M_{\xi_2}, M_{\eta_2}$ are equal to $2, 3$ or 4 and denote the Wang's integration order. The weighted function W_{mnrl} and the integration points ($\xi_1^m, \eta_1^n, \xi_2^r, \eta_2^l$ for quadrangles or $\tau_1^m, \zeta_1^n, \tau_2^r, \zeta_2^l$ for triangles) are listed in Reference [8]. Wang and Atalla [8] showed that results obtained for the fourth order are the most accurate. In the following, the numerical computations of singular integrals were done using $4 \times 4 \times 4 \times 4$ integration scheme. For non-singular integral, numerical results were obtained using $4 \times 4 \times 4 \times 4$ Gauss quadrature points.

5. NUMERICAL RESULTS

To demonstrate the accuracy and the efficiency of the present approach, several numerical applications are presented in this section. In the following, the accuracy of the extended method to triangles is examined for this integral:

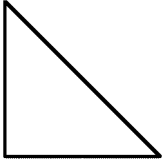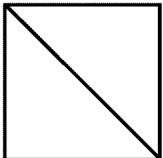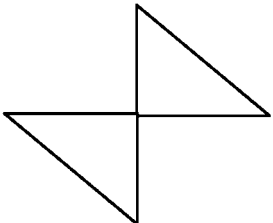$$I = \int_{S_1} \int_{S_2} \frac{1}{R} \, dS_1 \, dS_2 \qquad (21)$$

calculated directly on triangular master elements. The obtained results are summarized in Table I.

When the integration is evaluated on the same element, the error is about 1.7%. However, it is about 4.3% when the singularity is concentred at the common edge of two adjacent elements and it becomes very weak (less than 0.2%) when the elements have one node in common. From Table I, we can conclude that the presented method leads to good results, in particular, for the first and the last cases. For the second case, the error is relatively large compared to the other cases. This same behaviour has been observed by Hamdi when he evaluated semi-analytically the singular double integrals [1]. To reduce this error, he suggested evaluating the integral semi-analytically as he treated the first case. In what follows it will be seen that these errors do not affect dramatically the calculated acoustic pressure.

The radiation of a unit pulsating sphere is analysed using two BE models. The example of the sphere is selected because analytical solution is available and irregular frequencies can be predicted. In this second application, irregular frequencies are avoided and consequently no special treatment is needed.

The sphere has a radius of '$a = 1$ m'. It is excited by a unit velocity at frequency $f = 100$ Hz. It is surrounded by air ($\rho = 1.21$ Kg/m^3, $c = 343$ m/s). Two meshes are considered (Figure 3).

Table I. Numerical integration of Equation (21) using the presented method
in comparison with exact solution.

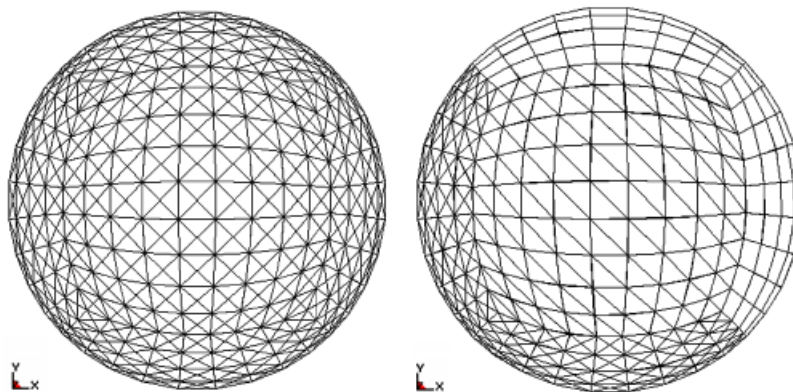|	Exact integration	Numerical integration
	1.0030	0.9853
	0.4835	0.5041
	0.26833	0.26838

Figure 3. Boundary element models of pulsating sphere mesh (1): 972 triangles;
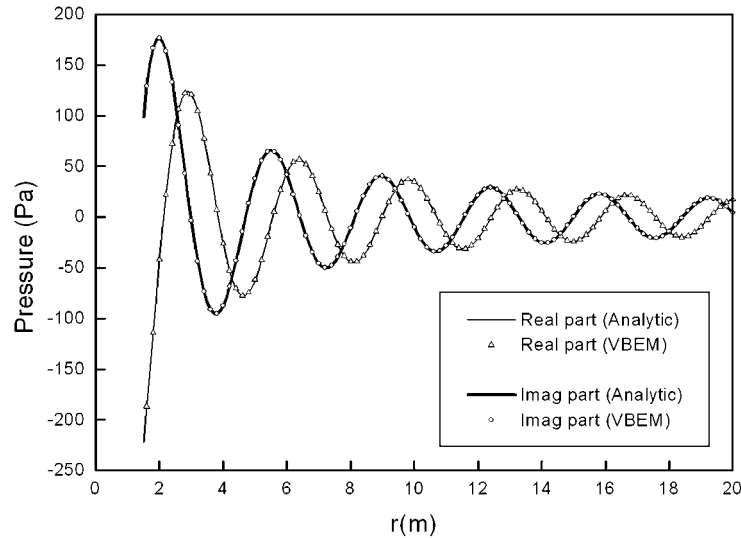mesh (2): 486 triangles and 243 quadratic elements.

Figure 4. Sound pressure radiated by pulsating sphere (mesh (1)).

The first one involves only triangular elements while the second contains both triangles and quadrangles.

Figure 4 depicts, for the first mesh, the variation of the radiated pressure with the radial distance computed analytically and by using VIBEM as presented in this paper. Good agreement is observed between numerical and analytical solutions. Even if mesh contains both triangles and quadrangles, the VIBEM is still in good agreement with the analytical solution (Figure 5).

In a third example, let us calculate the radiated pressure for different frequencies at a point located at $r = 4$ m from the sphere centre. From Figure 6, many peaks occur. They are related to the resonance of the interior volume of the sphere [11]. If we refine the mesh, the solution still does not converge and we will get non-physical resonances. These peaks do not have any physical meaning at the considered frequencies. Since the interior region resonates and since both interior and exterior problems share the same integral operator, the integral equation governing exterior problem should break down at the natural frequencies of the interior problem. To overcome this problem, it is necessary to discretize some additional elements inside the sphere on which the impedance boundary condition is prescribed in order to eliminate the highly resonant interior effects from the solution [12]. Away from irregular frequencies, the presented numerical result shows good correlation with analytical solution as seen in Figure 6. The numerical algorithm for solving irregular frequencies is not implemented yet in the code we developed to validate the presented the singular integration method. It is our goal to implement in the near future an algorithm to solve irregular frequencies problem. The treatment of this problem in case of VIBEM is described in details in Reference [13]. Users of the VIBEM with mixed quadrilateral and triangular elements need to take into consideration the irregular frequencies problem.
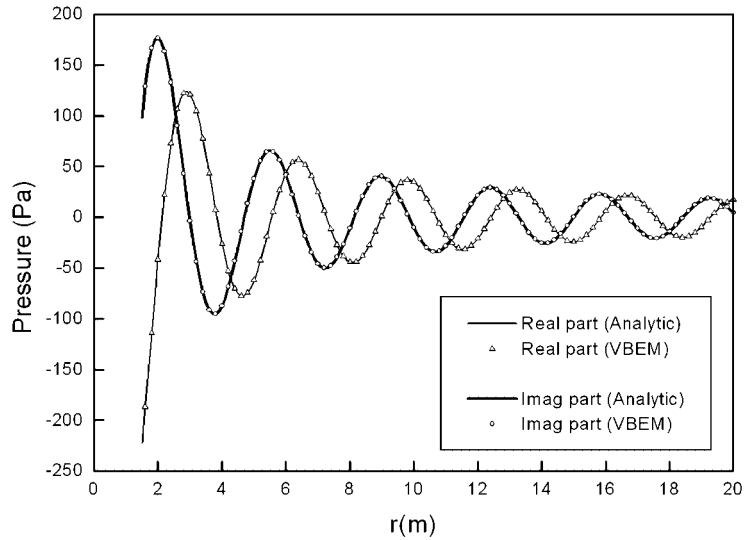
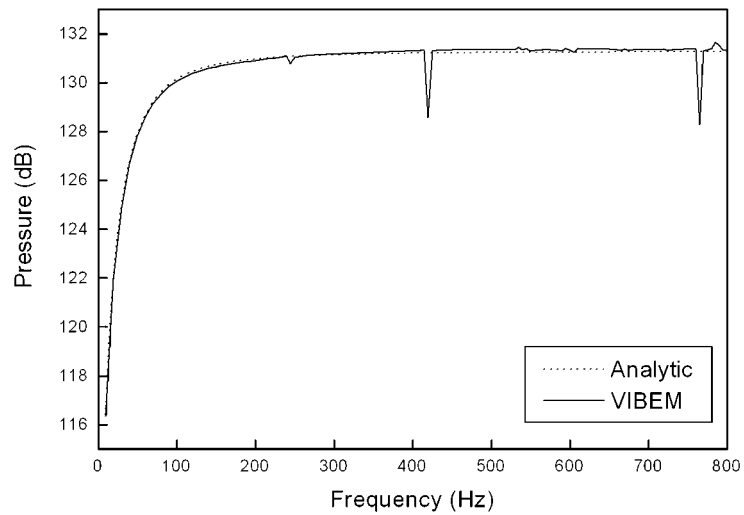Figure 5. Sound pressure radiated by pulsating sphere (mesh (2)).

Figure 6. Irregular frequencies effect on sound pressure radiated by unit pulsating sphere
for mesh (2) at a point situated at $r = 4$ m.

A parallelepiped box of $(1 \times 0.2 \times 0.2)\,\text{m}^3$ containing air was considered as a test example for interior problem. It was assumed that an end surface at $x = 0$ was vibrating as a rigid piston with a harmonic amplitude velocity of $1\,\text{m/s}$ at a frequency of $f = 200\,\text{Hz}$ whereas all other walls were rigid. In order to study the effect of the element aspect ratio on the results, the pressure field on the longitudinal axis were calculated for four meshes of element
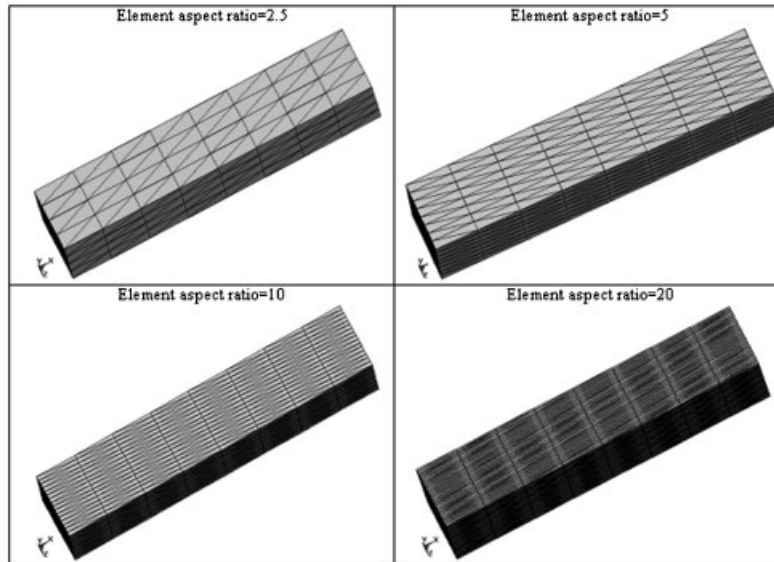
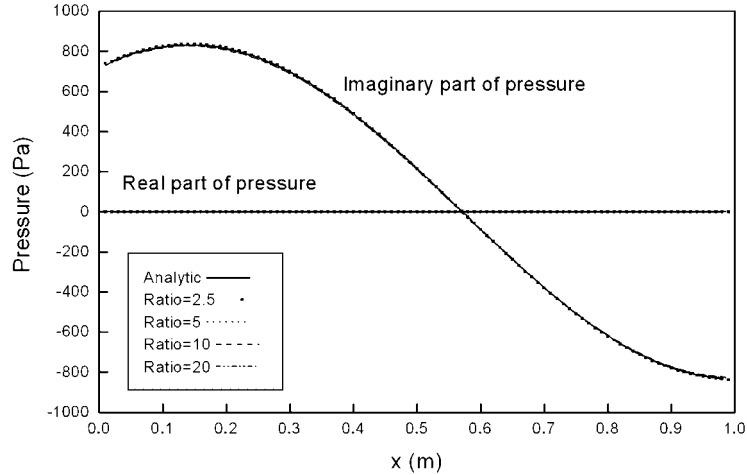Figure 7. BE models for different element aspect ratio.

Figure 8. Effect of the element aspect ratio on the acoustic pressure for $f = 200\,\mathrm{Hz}$.

aspect ratio of $2.5, 5, 10$ and 20 (Figure 7). It can be shown in Figure 8 that even for meshes involving large values of the element aspect ratio (10 for mesh 3 and 20 for mesh 4), the predicted pressure coincides with the exact theory. This indicates that the presented method is still applicable for meshes presenting large values of element aspect ratio.
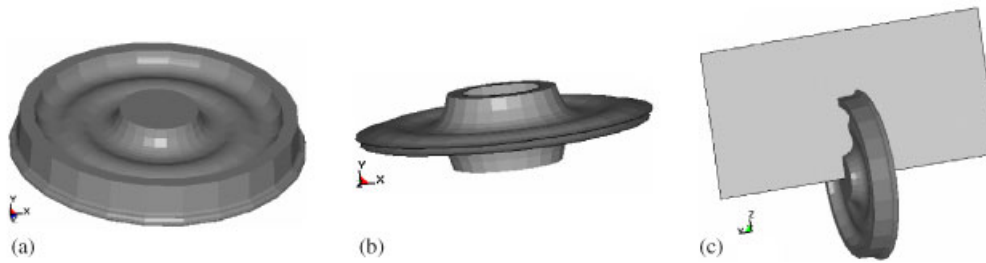
Figure 9. (a) Wheel model; (b) wheel surface on which the normal velocity is applied; and (c) plan on which the pressure is to be computed.
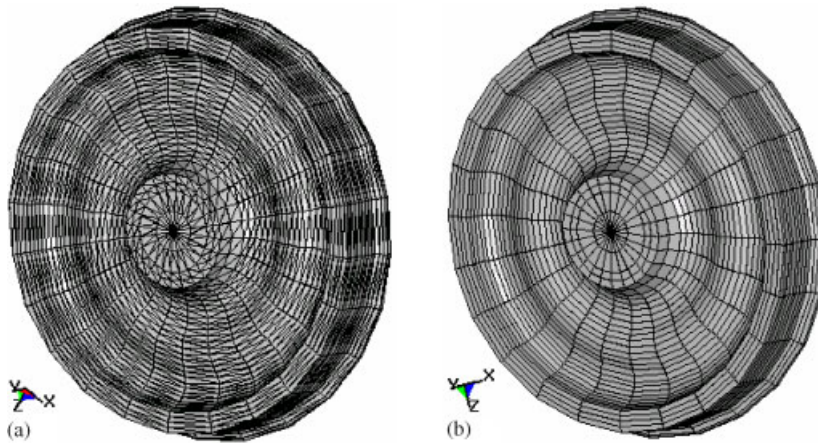

Figure 10. Wheel BE models (1946 nodes): (a) mesh (1) containing 3888 triangles; and (b) mesh (2) containing 1920 quadrangles and 48 triangles.

In order to check the efficiency of the presented method for complex geometry, radiation of a wheel using two BE models is analysed in this last application. The wheel (Figure 9(a)) is excited at a frequency $f = 200$ Hz by a normal velocity $V_n = 4 \times 10^{-3}$ m/s only applied on the surface shown in Figure 9(b). The remaining parts of the wheel are assumed to be perfectly rigid. The presented method is applied to calculate the pressure in the plane depicted in Figure 9(c). Both meshes, involving 1946 nodes, are shown in Figure 10. The first one contains 3888 triangular elements whereas the second is constituted by 1968 elements where 48 are triangular elements. In Figure 11, we presented the acoustic pressure radiated in interior and exterior wheel using both meshes (1) and (2). The two results compare well although the small difference in amplitude. This can be explained by the fact that mesh (1) is very fine compared to the second mesh.
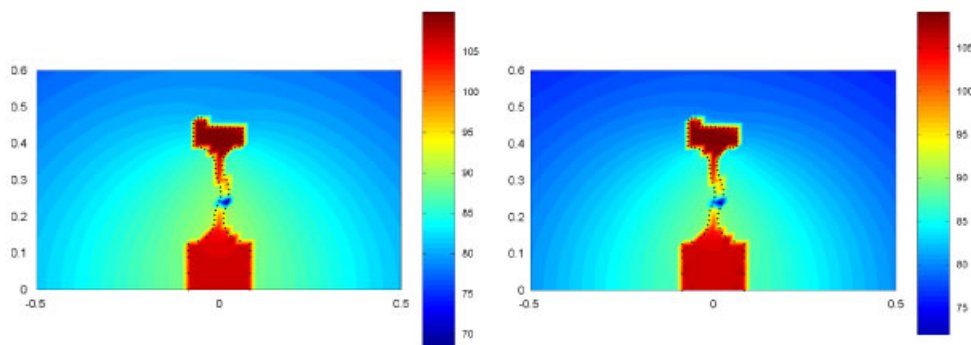
Figure 11. Pressure in dB calculated on plane by using (left) mesh (1), (right) mesh (2).

6. CONCLUSION

In this paper, the straightforward technique proposed by Wang and Atalla [8] for computing the singularity $1/R$ over quadrilateral element is extended to triangular one by using the generalized polar co-ordinates transformation presented by Wu [9]. Hence, this method can handle meshes involving both triangles and quadrangles without any special treatment of singularity. The integration method developed in this paper can be easily implemented in existing acoustic VIBEM codes in order to handle both quadrilateral and triangular elements in the same problem. Numerical examples demonstrating the efficiency of the extended method have been presented.

REFERENCES

 1. Hamdi MA. Formulation variationnelle par équations intégrales pour le calcul de champs acoustiques linéaires proches et lointains. *Ph.D. Thesis*, Université de technologie de Compiègne, 1982.
 2. Erchiqui F. Modélisation et simulation des interactions fluide structure par une méthode variationnelle couplant les équations intégrales et les éléments finis. *Ph.D. Thesis*, Université de Laval, Québec, 1994.
 3. Tournour M. Modélisation numérique par élément finis et éléments finis de frontière du comportement vibroacoustique de structures complexes assemblées et couplée à une cavité. *Ph.D. Thesis*, Université de technologie de Compiègne, 1999.
 4. Bonnet M, Maier G, Polizzotto C. Symmetric Galerkin boundary element method. *Applied Mechanics Reviews* 1998; **51**:669–704.
 5. Jeans R, Mathews IC. Solution of fluid structure interaction problems using a coupled finite element and variational boundary element technique. *Journal of Acoustical Society of America* 1990; **88**(5):2459–2466.
 6. Chen ZS, Hofstetter G, Mang HA. A symmetric Galerkin formulation of the boundary element method for acoustic radiation and scattering. *Journal of Computational Acoustics* 1997; **5**(2):219–241.
 7. Bajaj C, Xu G, Warren J. Acoustics scattering on arbitrary manifold surfaces. *Geometric Modelling and Processing*; *Theory and Applications*, July 10–12, 2002, Wako, Saitama, Japan.
 8. Wang W, Atalla N. A numerical algorithm for double surface integrals over quadrilaterals with a $1/R$ singularity. *Communications in Numerical Methods in Engineering* 1997; **13**:885–890.
 9. Wu TW. Three dimensional problems. *Boundary Element Acoustics*: *Fundamentals and Computer Codes*. WIT Press: Southampton, 2000; 51–67.
10. Chen JT, Hong HK. Review of dual boundary element methods with emphasis on hypersingular integrals and divergent series. *Applied Mechanics Reviews* 1999; **52**(1):17–33.
11. Chen JT, Chen KH, Chen IL, Liu LW. A new concept of modal participation factor for numerical instability in the dual BEM for exterior acoustics. *Mechanics Research Communications* 2003; **26**(2):161–174.
12. Estorff OV. *Boundary Elements in Acoustics*: *Advances and Applications*. WIT Press: Southampton, 2000; 51–67.
13. Zhang Z, Vlahopoulos N, Allen T, Zhang KY. A source reconstruction process based on an indirect variational boundary element formulation. *Engineering Analysis with Boundary Elements* 2001; **25**:39–114.